Harmonic Active Filtering and Impedance-based Stability Analysis in Offshore Wind Power Plants

Dhua, Debasish; Yang, Guangya; Zhang, Zhe; Kocewiak, ukasz Hubert; Timofejevs, Artjoms

Published in:
Proceedings of 16th Wind Integration Workshop

Publication date:
2017

Document Version
Peer reviewed version

Harmonic Active Filtering and Impedance-based Stability Analysis in Offshore Wind Power Plants

Debasish Dhua✉, Guangya Yang, Zhe Zhang
Department of Electrical Engineering
Technical University of Denmark
2800 Kgs. Lyngby, Denmark
✉ debasish.dhua@gmail.com

Łukasz H. Kocewiak, Artjoms Timofejevs✉
Department of Electrical Systems Analysis
DONG Energy Wind Power
2820 Gentofte, Denmark
✉ artti@dongenergy.dk

***Abstract*—Nowadays, to eliminate harmonics injected by the wind turbines in offshore wind power plants there is a need to install passive filters. Moreover, the passive filters are not adaptive to harmonic profile changes due to topology changes, grid loading etc. Therefore, active filters in wind turbines are proposed as a flexible harmonic mitigation measure. The motivation of this study is to explore the possibility of embedding active filtering in wind turbine grid-side converters without having to change the system electrical infrastructure. The active filtering method can prevent additional equipment installation and provides effectively similar functionality as passive filters. This work is focused on harmonic propagation studies in wind power plants, power quality evaluation at the point of connection and harmonic mitigation by active filtering. Finally, an impedance-based stability analysis of the grid-connected converter system is performed.**

Keywords-Active Filtering, Impedance-based Stability, Notch Filter, Offshore Wind Power Plant

I. INTRODUCTION

Nowadays, power electronics has become an integral part of wind power plants (WPPs). It provides efficient and regulated power flow under varying wind conditions. Moreover, the power electronic interfaces offer various functionality of wind turbines (WTs) such as voltage, frequency, active and reactive power control [1]. However, they provide the aforementioned control capability at the cost of additional harmonic distortion in the converter output voltage. Therefore, harmonics are of special concern for WPP developers, operators and utilities [2].

WPPs are being located more and more far from shore requiring the use of long HVAC submarine cables between offshore and onshore substations. The cable capacitance and the transformer inductances create multiple resonance points. The resonances, together with the harmonic emissions from WTs, can cause excessive distortion at the point of connection (POC) [3]. To eliminate the wide range of harmonics, the size of the passive filters becomes large and expensive. Moreover, the passive filters are not adaptive to any potential topology or system loading change. Therefore, controllable harmonic shaping by grid-tied converters seems to be an attractive alternative. Active filtering (AF) is not only adaptable to changes in harmonic profile but also provides flexible control without, in many cases, any additional equipment or extended component rating. AF in this paper is defined as basically any WT control functionality which leads to intentional harmonic distortion level improvement at the point of interest, e.g. extra noise rejection capability, harmonic emission reduction from internal non-linear components or controlled harmonic current injection. Active in this context means a control circuit comprising of active components, i.e. that transfers energy from its power supply to the load.

AF is usually used in shunt-connected grid-tied converters [4], [5], and the motivation of this study is to explore the possibility to embed AF in WT grid side converters. The idea is to shape the controller response to reduce the impact of resonances at the busbar of interest. This AF method may prevent having to install passive filters, and it can perform similarly as classical passive filters. This is critical for offshore systems where it may not be feasible to install passive filters due to e.g. to space restrictions, and high installation and maintenance cost.

II. SYSTEM OVERVIEW AND CONTROL DESIGN

The simplified diagram of the investigated offshore WPP is presented in Figure 1. It comprises four identical Type-4 WTs. The WTs are connected to the offshore MV array cable system via a step-up transformer. The POC is defined at the LV side of the offshore transformer (i.e. MV level). Furthermore, the WPP is connected to the onshore grid at the point of common coupling (PCC) via long HVAC cable. The WT model is simplified for the harmonic simulation purposes, i.e. the DC link circuit is represented as a constant DC voltage source. The modelled part of the WPP is marked with red dotted line in Figure 1.

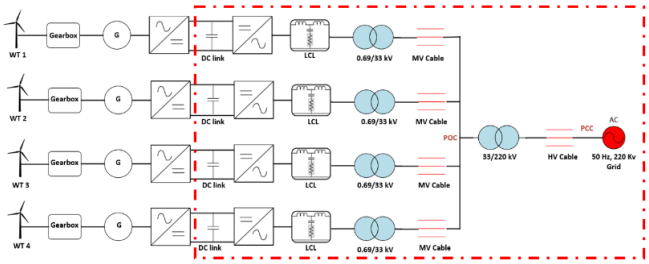

Figure 1 Simplified diagram of the investigated offshore wind power plant.

A. System Parameters

A simplified WPP electrical infrastructure is modelled in Matlab/Simulink to represent harmonic propagation and

estimate harmonic distortion at the POC. The model includes the DC voltage source, 3-phase 2-level converter bridge, passive LCL filter [6], step-up transformer, MV array cable network, offshore transformer, HV transmission cable [7], and a simplified external electrical network. More details about the modelled components can be found in Table 1.

Table 1 System components and corresponding parameters.

System component	Parameters
Grid-tied converter with SPWM	2-level, 3-phase, IGBT-diode, Turn on delay = 5μs
DC link voltage	1.5kV
LCL filter (per phase)	L_{inv} = 0.14mH, L_{grid} = 0.012mH, C_f = 2000μF, R_f = 0.025Ω
Wind turbine transformer (0.69/33kV)	10MVA, R = 0.004p.u., L = 0.0415p.u.
33kV MV cable (per phase/km)	L = 0.55mH, C = 0.26μF, R = 0.05Ω
Offshore transformer (33/220kV)	50MVA, R = 0.004p.u., L = 0.0415p.u.
220kV HV cable (per phase/km)	L = 0.75mH, C = 0.14μF, R = 0.04Ω
Grid	220kV ($V_{RMS, L-L}$), 3-phase, 50Hz

WPP electrical infrastructure components (i.e. cables and transformers) create resonances and, therefore, have a significant impact on harmonic distortion. In this study, the submarine MV cable length is varied to reflect potential resonance profile variation due to possible topology changes. Furthermore, the harmonic voltage and current distortion is estimated for the system.

It can be seen from the Bode plot in Figure 2 that the resonance frequency is at 6.68×10^3 rad/second. Additional damping resistance allows to reduce the resonance gain. Moreover, the attenuation of the LCL-filter is seen to become gradually higher for higher order harmonics.

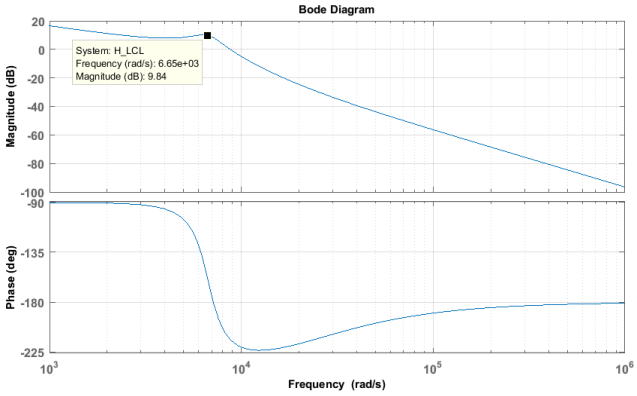

Figure 2 Bode plot of the wind turbine LCL passive filter.

B. Wind Turbine Converter Control

The WT control is based on the synchronous reference frame current control scheme. The voltage $v(t)$ and current $i(t)$ are expressed in the dq reference frame with their corresponding direct axis and quadrature axes components as in Equation (1)

$$v(t)=\left(v_d(t)+jv_q(t)\right)$$
$$i(t)=\left(i_d(t)+ji_q(t)\right) \quad (1)$$

$$P(t)=\frac{3}{2}\left[v_d(t)i_d(t)-v_q(t)i_q(t)\right]$$
$$Q(t)=\frac{3}{2}\left[v_d(t)i_q(t)+v_q(t)i_d(t)\right] \quad (2)$$

To control the output power, active power reference (P_{ref}) and reactive power reference (Q_{ref}) can be rewritten from Equation (2) with setting the V_q signal to 0 in the phase locked loop (PLL).

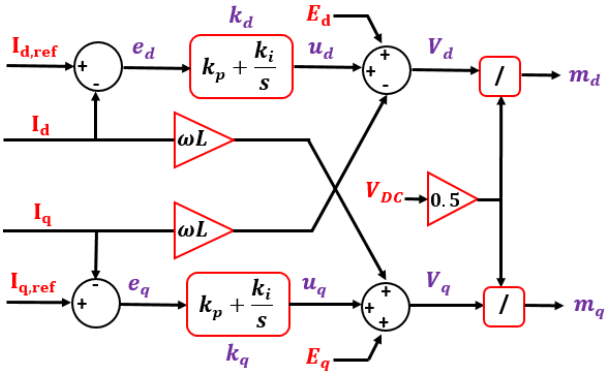

Figure 3 Current controller in the synchronous reference frame.

To generate the $I_{d,ref}$ and $I_{q,ref}$ from P_{ref} and Q_{ref} signals, the voltage signals (E_d and E_q) are used. These are measured in the WT LV circuit as indicated in Figure 4. The voltage signals are transformed then into the dq reference frame using PLL ($E_d = E_{d,DC} + E_{d,AC}$ and $E_q = E_{q,DC} + E_{q,AC}$); where, $E_{d,DC}$ contains the voltage corresponding to the fundamental frequency (50Hz) and $E_{d,AC}$ refers to the voltage of higher order harmonic frequencies. Therefore, to pass only the DC component in the dq reference frame the voltage signals are passed through the lowpass filter (LF).

The entire WT control scheme (including control blocks, modulation block, passive components, converter, measurements) is shown in Figure 4.

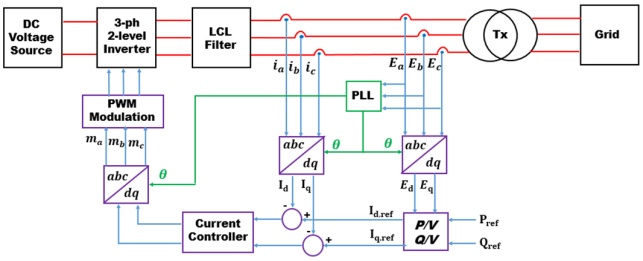

Figure 4 Wind turbine grid-tied converter overall control strategy.

The WT current controller (as in Figure 3) utilizes proportional-integral (PI) regulators to track $I_{d,ref}$ and $I_{q,ref}$ reference signals, furthermore, grid voltage feedforward is also included. The open-loop and closed-loop controller frequency responses are presented in Figure 5 and Figure 6, respectively. The PI controller parameters are determined by using Matlab/PID Tool for the open-loop system $H(s)$ as defined in Equation (3) and set to $k_p = 0.17$ and $k_i = 71$, where $H_{PI}(s)$ is the PI controller transfer function, $H_{delay}(s)$ is the overall control delay and $H_{LCL}(s)$ is the LCL-filter transfer function based on the current feedback as presented in Figure 4. The WPP grid is not included in the basic WT controller tuning.

$$H(s)=H_{PI}(s)H_{delay}(s)H_{LCL}(s) \quad (3)$$

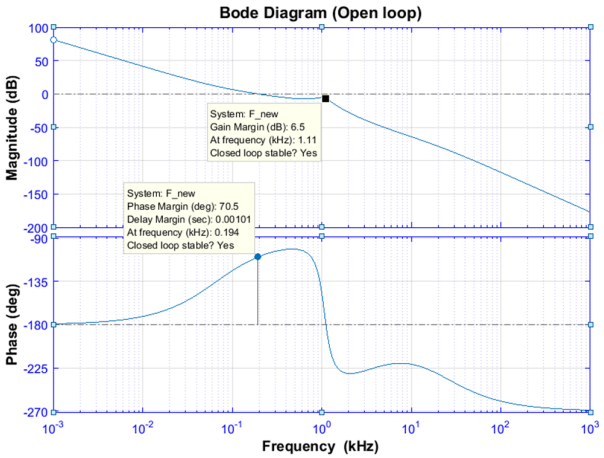

Figure 5 Bode plot of the open-loop transfer function.

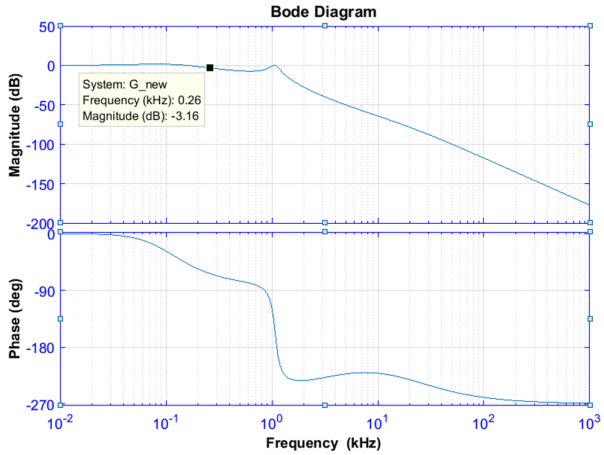

Figure 6 Bode plot of the closed-loop transfer function.

From the open-loop and closed-loop frequency responses the following characteristics of the current controller are [8], [9] (i) the open loop gain margin (GM) > 6dB, (ii) phase margin (PM) >45°, (iii) closed-loop bandwidth > 0:25 kHz.

III. Simulation Studies

A. Fundamental Frequency Control

To obtain WPP steady state operation all four WTs are turned on one after another with an interval of 0.5s. The WTs are triggered by setting the active power reference (P_{ref}) value to the nominal value of 6MW. For simplification, no ramping up slope is introduced. The WT line current and voltage are shown in Figure 7 and Figure 8 respectively.

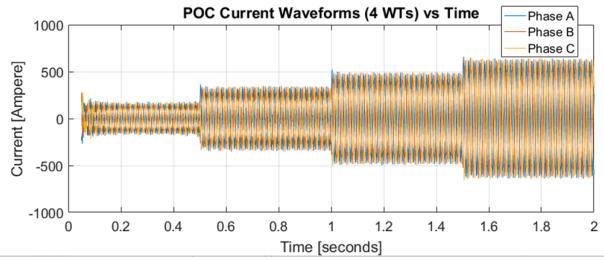

Figure 7 Current waveform showing wind turbine connection measured at the point of connection.

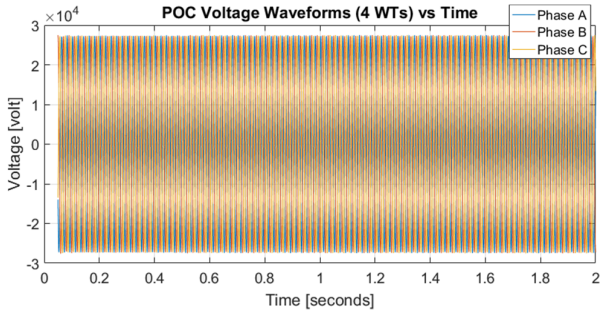

Figure 8 Voltage waveform measured at the point of connection.

In Figure 9, the active power level is rising in steps from 6MW to 24MW as the number of connected WTs is increasing. Whereas, the reactive power level is kept always at zero MVAr during the whole simulation to maintain unity power factor at the POC. Figure 7 shows increasing current injection to the POC. The first few waveform cycles are neglected to omit the transient behaviour at the beginning of the simulation.

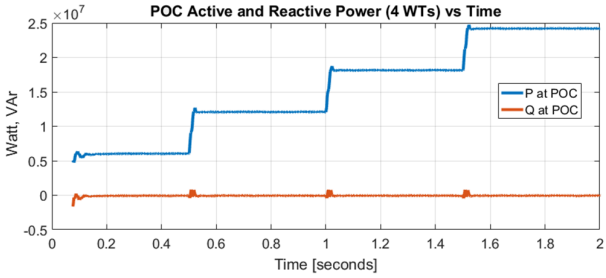

Figure 9 Active and reactive power changes at the point of connection while new wind turbines are connected.

B. Harmonic Simulations

The next step is to evaluate the harmonic content by applying Fourier analysis on the steady state voltage and current waveforms. For the four-WT system (as shown in Figure 1) the voltage and current total harmonic distortion (THD) is measured using the fast Fourier transform (FFT) block (from Matlab/Powergui block) and listed in Table 2. Based on the simulations it can be seen that the current harmonics content is gradually decreasing with connection of more and more WTs which can be explained as overall system damping increase.

Table 2 Harmonic distortion at the point of connection depending on number of wind turbines in operation.

Number of WTs	THD_V at POC	THD_I at POC
1 (WT_1)	0.34	15.95
2 (WT_1+WT_2)	0.50	15.13
3 (WT_1+WT_2+WT_3)	0.47	9.50
4 (WT_1+WT_2+WT_3+WT_4)	0.49	7.44

Figure 10 shows how the parallel resonance at the POC can vary when the number of WT connected within the WPP offshore network is increasing. The resonance peak is decreasing gradually as well as the harmonic current distortion (see Table 2).

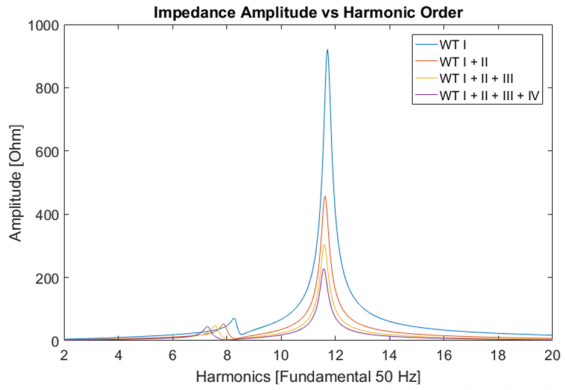

Figure 10 Impedance plot (and damping) variation at the point of connection depending g on number of wind turbines in operation.

Typically, the voltage harmonic content is of concern at the transmission level since the voltage is maintained across the wide interconnection area whereas the current level can vary while flowing through multiple branches within the meshed area. In this study, the voltage THD (at 33kV) is desired to be kept close to 0.2%. This value is a fraction of the Planning Levels from IEC 61000-3-6 and is realistic Grid Code requirements. Thus, in this study AF is going to be introduced to lower the THD levels presented in Table 2.

C. Array Cable Length Variation

The impact of the WPP electrical infrastructure components on the resonance profile [10] is presented in this part. The array cable length is varied (Case 1: 50km, Case 2: 31.5km and Case 3: 24km) while the HV export cable length is constant (50km). Figure 11 shows the simplified system topology which was used in the study. It can be seen in Figure 12 that the main resonance frequency at the POC can change significantly when the total system capacitance is changed which can be caused by disconnecting e.g. one array cable string.

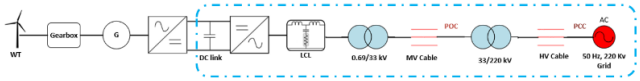

Figure 11 Simplified system with only one wind turbine defined to investigate the impact on array cable length on harmonic distortion.

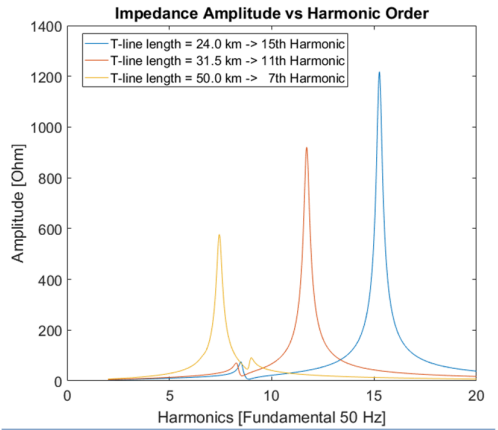

Figure 12 Impedance profile, seen at the point of connection, which varies depending on array cable length.

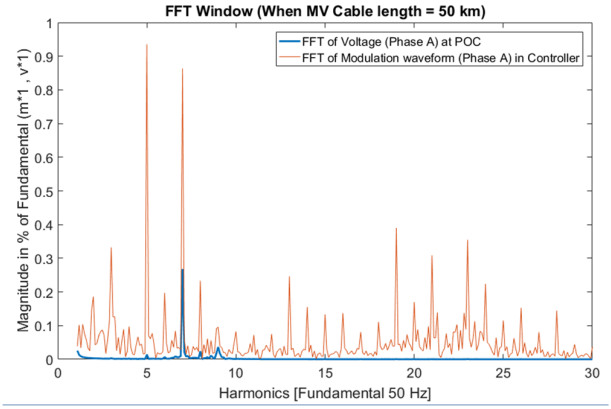

Figure 13 Fourier decomposition of the normalized voltage at the point of connection as well as command signal in the controller (Case 1, cable length: 50km).

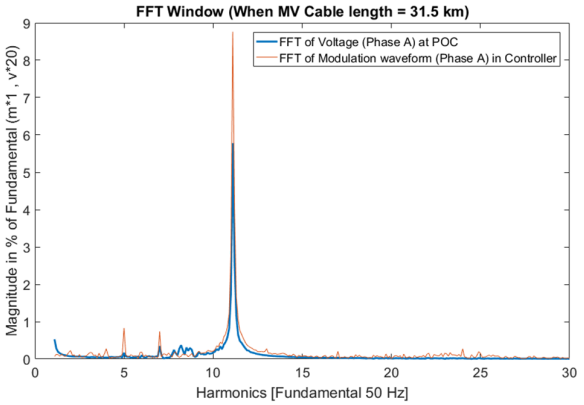

Figure 14 Fourier decomposition of the normalized voltage at the point of connection as well as command signal in the controller (Case 2, cable length: 31.5km).

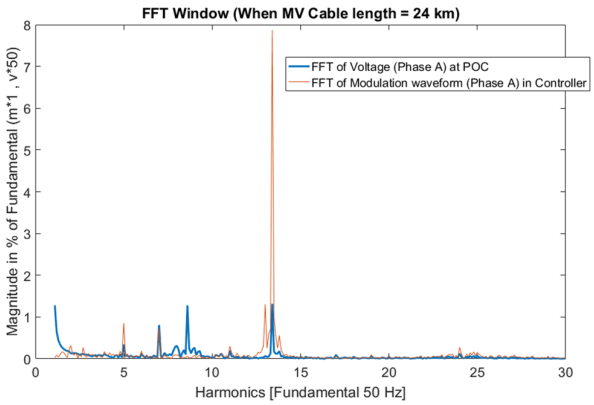

Figure 15 Fourier decomposition of the normalized voltage at the point of connection as well as command signal in the controller (Case 3, cable length: 24km).

When the MV cable length is changed, the resonance frequency is shifted and consequently the dominant harmonic frequency is different. The voltage at the POC as well as the output signal in the current controller have the same most prominent harmonics as presented in Figure 13, Figure 14 and Figure 15. It shows that the resonance impact can be seen at the POC as well as within the WT LV power circuit where the current feedback is placed (see Figure 4). It is, however, believed that in more complicated systems the resonances are different at different busbars. It also indicates that the WT

control can influence the harmonic distortion level if appropriately adjusted.

The control signals are also contaminated with the system harmonics due to the controller low harmonic rejection capability. This can be improved by using appropriate AF techniques. AF in this paper is defined as any additional WT control feature which can change the harmonic distortion level by e.g. extra noise rejection capability, harmonic emission reduction or controlled harmonic current injection.

IV. Active Filtering for Wind Power Plant Harmonic Mitigation

The proposed AF solution is quite straight forward to implement in the existing WT control. The voltage is measured at the LV side of the WT transformer (just after the LCL filter) and passed through the low-pass filter. Typically, the filters are digitally implemented in the control chain. Buttherworth, Chebyshev, Bessel, Elliptical filters are commonly used for harmonic noise attenuation. To simplify the analysis, during the design and in the simulation model the filters are implemented in the Laplace domain (i.e. *s*-domain). Butterworth LF and Butterworth notch filter (NF) are used to eliminate the harmonics from the voltage and current waveforms. The modulation (command) waveforms given by the controller (see Figure 3 and Figure 4) are in the *abc* reference frame and are passed through the NF to attenuate a specific harmonic order from the controller output signal.

A. Active Filter Design

LFs and NFs with corresponding signals are shown in Figure 16 and Figure 17. The proposed AF scheme comprises of LF and NF.

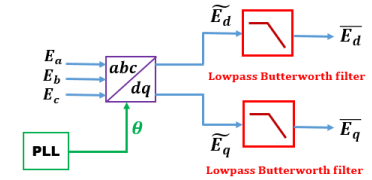

Figure 16 Lowpass Butterworth filter placement in the wind turbine control chain.

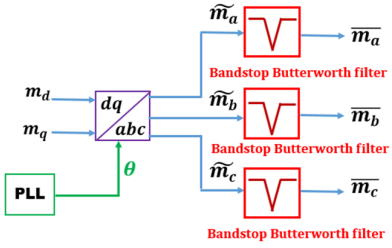

Figure 17 Butterworth notch filter placement in the wind turbine control chain.

The LF cut-off frequency is set to 10Hz, since the DC component (0Hz) of voltage signals in the *dq* frame is only processed. Whereas, the NF characteristics are decided by the resonance frequency that needs to be eliminated from the modulation waveform. The NF can be represented as

$$H_{NF}=\frac{s^2+\omega_c^2}{s^2+\zeta s+\omega_c^2} \quad (4)$$

Where, ω_c is the resonance frequency and ζ defines the attenuation of the NF. The open-loop control system with the NF is shown below in Figure 18.

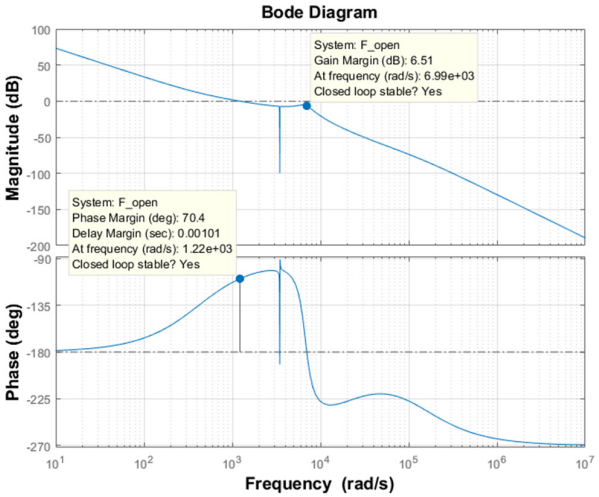

Figure 18 Bode plot of wind turbine converter control including the notch filter.

B. Single Wind Turbine Implementation

Firstly, the proposed AF was tested/simulated on a system presented in Figure 11. For example, 31.5km MV cable capacitance is causing a resonance at the POC close to the 11th harmonic (see to Figure 12). Thus, the NF resonance frequency is set to eliminate the 11th harmonic. It can be seen based on the open-loop Bode magnitude plot that the controller can selectively attenuate the 11th harmonic component (see Figure 18). It is important to note that the NF response shown in the Bode plot represents the ideal condition (- 100dB). In reality, a limited attenuation can be caused by the nonidealities, e.g. digital implementation, sampling resolution.

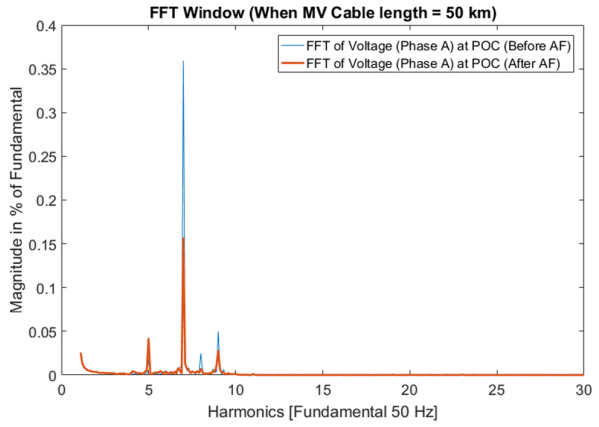

Figure 19 Harmonic spectrum of the point of connection voltage with and without active filtering (Case 1, cable length: 50km).

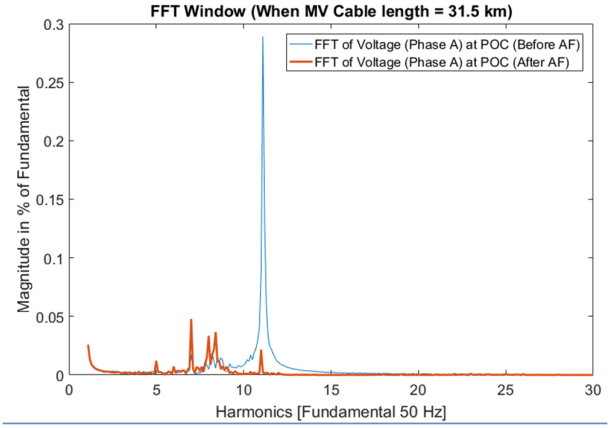

Figure 20 Harmonic spectrum of the point of connection voltage with and without active filtering (Case2, cable length: 31.5km).

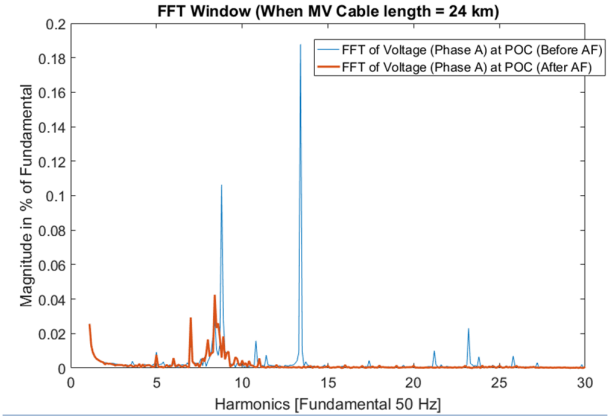

Figure 21 Harmonic spectrum of the point of connection voltage with and without active filtering (Case 3, cable length: 24km).

After inserting the filters (i.e. LF and NF) in the control chain, the simulations were run again. From Figure 19, Figure 20, and Figure 21 it can be seen that NF is capable of effectively and selectively reducing the harmonic content at the POC. In all three cases, the NF is adjusted and successfully eliminating the major harmonic components as presented in Table 3.

Table 3 Active filtering effectiveness at the point of connection (single wind turbine study).

Case	THD_I		THD_V	
	with AF	w/o AF	with AF	w/o AF
Case 1, (50km)	13.27	7.83	0.50	0.18
Case 2, (31.5km)	21.11	2.49	0.35	0.09
Case 3, (24km)	23.88	1.61	0.23	0.08

C. Wind Power Plant Implementation

Secondly, the proposed AF solution was implemented on the WPP level to observe the performance of NFs in a multiple WT system. The WTs are connected to the POC via MV cable with different cable lengths (i.e. 50km, 31.5km and 24km). The NFs are tuned accordingly to reflect local resonance profiles as shown in Figure 12. The THD estimation after applying AF (i.e. LFs and NFs) is presented in Table 4.

Table 4 Active filtering effectiveness at the point of connection (wind power plant study).

Connected WTs	THD_I		THD_V	
	with AF	w/o AF	with AF	w/o AF
WT_1	28.98	7.61	0.42	0.24
WT_1+WT_2	13.67	3.85	0.44	0.24
WT_1+WT_2+WT_3	11.67	2.75	0.53	0.26

Based on the results it can be seen that the implementation of LFs and NFs in WT control chain is reducing the harmonic distortion level in the WPP offshore electrical system.

V. Harmonic Small-Signal Stability Studies

A. Wind Turbine Control and Active Filtering Transfer Function

The WT converter control frequency response is modified after inserting the NF and the Equation (3) is rewritten as shown in Equation (5). The NF transfer function is represented as $H_{NF}(s)$,

$$H_{new}=H_{PI}(s)H_{delay}(s)H_{LCL}(s)H_{NF}(s) \quad (5)$$

From the Bode plot (Figure 18) and the Nyquist diagram (Figure 22) the stability of the system with the NF is verified with GM of 6 dB and PM of 70°. Therefore, the robust AF solution is provided which effectively reduces the harmonic distortion at the POC. It is worth to emphasize that no additional passive filters across the WPP electrical infrastructure are needed. In practice, the AF can be digitally implemented after the A/D signal conversion and before the modulation block inside the WT converter control loop.

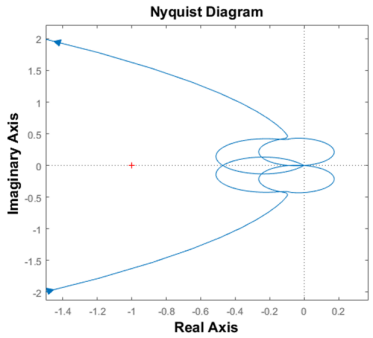

Figure 22 Nyquist diagram of the open-loop control with the notch filter.

B. System Impedance-based Stability Analysis

The impedance-based stability analysis was used to evaluate the robustness of the WT converters with AF on a system level. Taking into consideration the complex WPP electrical infrastructure the small-signal stability was evaluated at the POC.

1) Theoretical background

The impedance-based stability analysis can be easily and successfully applied in WPP systems [11], [12]. The WT is represented as a Norton equivalent circuit and the grid is represented as a Thévenin circuit as presented in Figure 23.

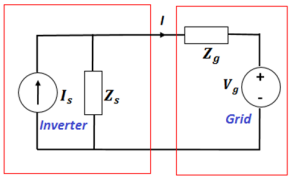

Figure 23 Simplified wind power plant small-signal representation used in impedance-based stability analysis.

The current flowing from the WT to the grid can be described as

$$I(s)=\frac{I_s(s)Z_s(s)}{Z_s(s)+Z_g(s)}-\frac{V_g(s)}{Z_s(s)+Z_g(s)} \quad (6)$$

which can be reconfigured as

$$I(s)=\left[I_s(s)-\frac{V_g(s)}{Z_s(s)}\right]\frac{1}{1+Z_g(s)/Z_s(s)} \quad (7)$$

For the stability analysis, voltage source is assumed to be stable when unloaded, the load current is stable when it is grounded; hence the stability criterion depends on the transfer function [13],

$$H(s)=\frac{1}{1+Z_g(s)/Z_s(s)} \quad (8)$$

To estimate the harmonic small-signal stability of the WT grid-tied converter system, the GM and PM of the impedance frequency characteristic play the key role. Therefore, the conclusions from the small-signal stability analysis can also be extended for large interconnected system [14]:

- Magnitude plot: The intersection of the WT and grid impedance frequency characteristic (which relates to the system open-loop transfer function) correlates to the dominant harmonic frequency in the measured inverter output voltage and current.
- Phase plot:

$$\Phi_{margin}=180^{\circ}-\left|\Phi_{converter}-\Phi_{grid}\right| \quad (9)$$

The larger the phase difference between the WT and grid phase responses, the lower the PM.

2) System-level implementation

This section shows the application of the impedance-based stability analysis on the WPP level. It is assumed that four MV networks (each representing one WPP) are connected to the same onshore transformer at the PCC via HVAC cables. Each WPP consists of four WTs interconnected at the POC.

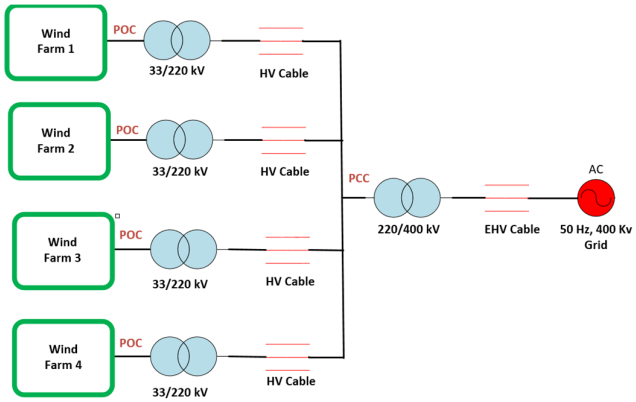

Figure 24 Wind power plant simplified diagram which was used for impedance-based stability analysis.

WF_1 and the grid impedance plots are presented in Figure 25. The MV cable length is 31.5km for all WTs within WF_1,

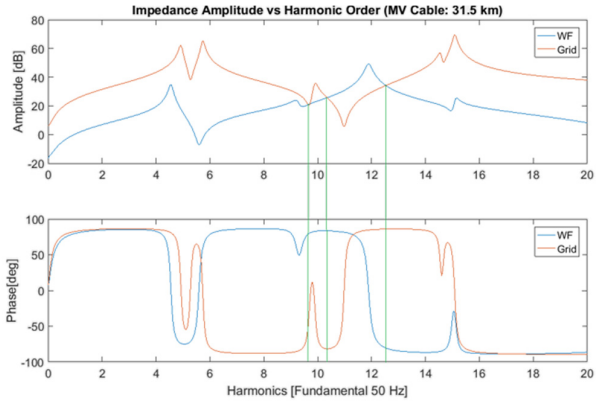

Figure 25 Impedance plots seen at the point of connection.

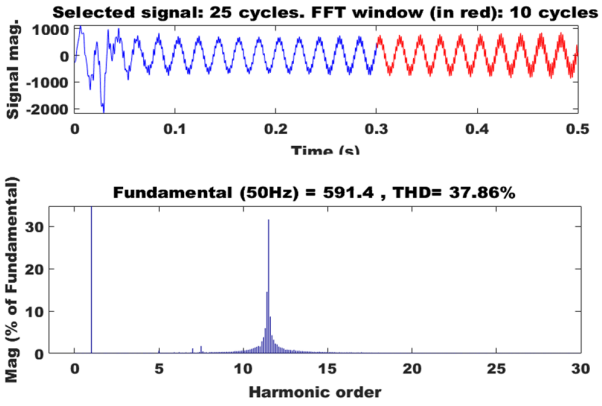

Figure 26 Current harmonic spectrum at the point of connection.

It can be seen in Figure 25 and Figure 26 that the resonance peak in the harmonic spectrum is corresponding to the frequency where the WF_1 impedance magnitude plot intersects with the grid impedance magnitude plot. Furthermore, the closed-loop PM is also quite small, i.e. less than 30°, and around the 11th harmonic which is also identified from FFT plot in Figure 26. To illustrate the impact of the PM obtained from impedance-based stability analysis on the THD level few more study cases were investigated as listed in Table 5.

Table 5 The impact of system damping on phase margins seen at the point of connection.

Cases	Damping	Φ_m	THD_I	Remark
R=0.1Ω	High	45°	1.77	Stable
R=0.01Ω	Moderate	35°	4.92	Stable with disturbance
R=0.001Ω	Low	15°	276.7	High disturbance

From Table 5 one can see how the PM is decreasing when the MV cable resistance is reduced (from 0.1 to 0.001Ω). Such extreme low value is used to show drastic changes in the harmonic profile (i.e. THD_I=276.7%). Simultaneously, harmonic distortion is increasing with the decrease of the MV cable damping. The lower resistance value, the higher THD at the POC.

VI. Conclusion and Future Work

The studies show the theoretical investigation of WPP harmonic propagation and AF implementation as a flexible and robust harmonic mitigation measure. The following was concluded:

- WT grid-tied converters can be used to effectively control the active and reactive power flow to the grid;
- It is possible to integrate AF inside the WT grid converter by using analog (in *s*-domain);
- The WPP existing resonance profile can be determined and used for AF tuning to reduce the harmonic contamination in the system;
- To tune the AF satisfactorily, it is essential to have the knowledge about the resonance profile of the WPP network;
- Impedance-based stability analysis can be applied to WPP systems.

The studies presented in this paper brings better understanding regarding WPP active harmonic mitigation techniques. However, the following future work is needed:

- Further AF development and optimization is needed addressing such aspects as digital control, e.g. digital filter (in *z*-domain);
- Adaptive AF can be developed based on an iterative algorithm adjusting according to electrical system topology changes (e.g. switching of array cables);
- The more extended impedance-based stability analysis is needed to understand the robustness of the proposed control strategy;
- The developed study can be tested in hardware prototyping and even further in real-life.

VII. Acknowledgment

The authors would like to express their appreciation to Mohammad Kazem B. Dowlatabadi and Troels Stybe Sørensen from DONG Energy Wind Power who provided valuable inputs to the analysis.

VIII. References

[1] R. D. Shukla, R. Tripathi and S. Gupta, "Power electronics applications in wind energy conversion system: A review," in *IEEE International Conference on Power, Control and Embedded Systems*, Allahabad, India, 29 November - 1 December 2010.

[2] O. Anaya-Lara, N. Jenkins, J. Ekanayake, P. Cartwright and M. Hughes, Wind energy generation: modelling and control, John Wiley & Sons, 2011.

[3] S. Jiang, S. Zhang, X. Lu, B. Ge and F. Z. Peng, "Resonance issues and active damping in HVAC grid-connected offshore wind farm," in *IEEE Energy Conversion Congress and Exposition*, Denver, CO, USA, 15-19 September 2013.

[4] F. Soares dos Reis, J. A. Villar Alé, F. Daher Adegas, R. Tonkoski Jr, S. Slan and K. Tan, "Active Shunt Filter for Harmonic Mitigation in Wind Turbines Generators," in *IEEE Power Electronics Specialists Conference*, Jeju, Korea, 18 - 22 June 2006.

[5] A. Luo, S. Peng, C. Wu, J. Wu and Z. Shuai, "Power electronic hybrid system for load balancing compensation and frequency-selective harmonic suppression," *IEEE Transactions on Industrial Electronics,* vol. 59, no. 2, p. 723–732, 2012.

[6] A. Kahlane, L. Hassaine and M. Kherchi, "LCL filter design for photovoltaic grid connected systems," in *Revue des Energies Renouvelables*, Ghardaïa, 2014.

[7] Nexans, "Submarine power cables," Nexans Deutschland GmbH, Hannover, 2013.

[8] M. Liserre, F. Blaabjerg and R. Teodorescu, "Grid Impedance Estimation via Excitation of LCL-Filter Resonance," *IEEE Transactions on Industry Applications,* vol. 43, no. 5, pp. 1401 - 1407, 24 September 2007.

[9] M. Liserre, A. Dell'Aquila and F. Blaabjerg, "Design and control of a three-phase active rectifier under non-ideal operating conditions," in *IEEE IAS Annual Meeting. Conference Record of the Industry Applications Conference*, Pittsburgh, PA, USA, 13-18 October 2002.

[10] Ł. H. Kocewiak, B. Laudal Øhlenschlæger Kramer, O. Holmstrøm, K. Høj Jensen and L. Shuai, "Resonance Damping in Array Cable Systems by Wind Turbine Active Filtering in Large Offshore Wind Power Plants," *IET Renewable Power Generation,* vol. 11, no. 7, pp. 1069-1077, 6 July 2017.

[11] X. Chen and J. Sun, "A study of renewable energy system harmonic resonance based on a DG test-bed," in *IEEE Applied Power Electronics Conference and Exposition*, Fort Worth, TX, USA, 6-11 March 2011.

[12] X. Wang, F. Blaabjerg and P. Chiang Loh, "An impedance-based stability analysis method for paralleled voltage source converters," in *International Power Electronics Conference*, Hiroshima, May 2014.

[13] M. Cespedes and J. Sun, "Impedance Modeling and Analysis of Grid-Connected Voltage-Source Converters," *IEEE Transactions on Power Electronics,* vol. 29, no. 3, pp. 1254-1261, March 2014.

[14] C. Buchhagen, M. Greve, A. Menze and J. Jung, "Harmonic Stability – Practical Experience of a TSO," in *The 15th International Workshop on Large-Scale Integration of Wind Power into Power Systems as well as Transmission Networks for Offshore Wind Farms*, Vienna, Austria, November 15-17, 2016.